ACS central science

http://pubs.acs.org/journal/acscii

Outlook

Application of Crystalline Matrices for the Structural Determination of Organic Molecules

Ashley D. Cardenal and Timothy R. Ramadhar*

Cite This: *ACS Cent. Sci.* 2021, 7, 406−414

Read Online

ACCESS | Metrics & More | Article Recommendations

ABSTRACT: While single-crystal X-ray diffraction (SC-XRD) is one of the most powerful structural determination techniques for organic molecules, the requirement of obtaining a suitable crystal for analysis limits its applicability, particularly for liquids and amorphous solids. The emergent use of *preformed* porous crystalline matrices that can absorb organic compounds and stabilize them via host−guest interactions for observation via SC-XRD offers a way to overcome this hindrance. A topical and current discussion of SC-XRD in organic chemistry and the use of preformed matrices for the *in crystallo* analysis of organic compounds, with a particular focus on the absolute structure determination of chiral molecules, is presented. Preformed crystalline matrices that are covered include metal−organic frameworks (MOFs) as used in the crystalline sponge method, metal−organic polyhedra (MOPs, coordination cages), porous organic materials (POMs)/porous organic molecular crystals (POMCs), and biological scaffolds. An outlook and perspective on the current technology and on its future directions is provided.

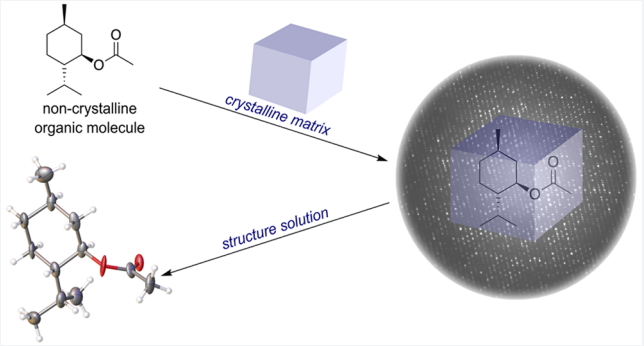

INTRODUCTION

The adage "*a picture is worth a thousand words*" is no less apt in organic chemistry and chemical biology: from glancing at a thin-layer chromatography plate to judge separation in flash chromatography, to observing an agar plate from a disk-diffusion assay to gauge natural product cidal activity, to using confocal microscopy to see probe localization in a cell. The most accessible method to empirically view a molecule is single-crystal X-ray diffraction (SC-XRD), which offers an indirect picture from modeling a molecule using an electron density map. SC-XRD is a valuable method for the structural elucidation of organic molecules; however, a bottleneck is the need for a suitable crystal. A promising strategy to circumvent this issue involves using preformed porous crystalline matrices to absorb analytes for SC-XRD (Figure 1).[1−3] We present background and coverage on preformed crystalline matrices for organic structure determination from an end user vantage point. We also provide a forward-looking perspective that promotes method development to bolster the potential of using these matrices as a first-line technique for structural determination and encourages researchers to leverage this approach.

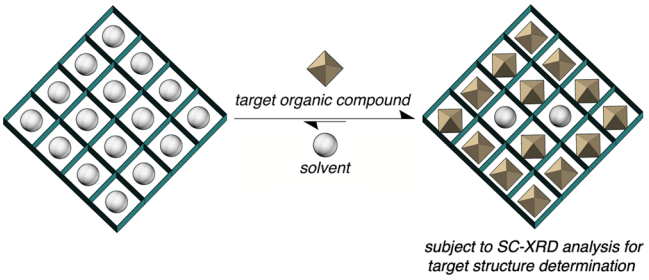

Figure 1. General strategy for determining the structure of organic molecules through the use of preformed crystalline matrices.

CRYSTALLOGRAPHY OF ORGANIC MOLECULES: A PRIMER

Routine methods for determining organic molecular structure include infrared spectroscopy (IR), mass spectrometry (MS), and the workhorse: nuclear magnetic resonance (NMR)

Received: November 2, 2020
Published: February 17, 2021

spectroscopy. However, a limitation of conventional NMR experiments is that spectral analysis is subject to human biases and error, leading to the dissemination of incorrect structures and publication of structural revision articles. Efforts to improve the robustness of NMR analysis involve an innovative combination of computer-assisted structure elucidation (CASE)[4] with anisotropic NMR data analysis [i.e., comparing experimental residual dipolar coupling (RDC) and residual chemical shift anisotropy (RCSA) values obtained from samples in a gel matrix with values from density functional theory (DFT) calculations].[5] Depending on molecular size and flexibility, however, the requisite DFT calculations may be computationally expensive. While NMR, IR, and MS deliver pieces of a structural puzzle, SC-XRD is the only gold standard method that can reveal the full structure—including relative and absolute configuration—in one experiment. Unlike most macromolecular SC-XRD experiments, the crystallographic "phase problem" for small molecules can be handled via *ab initio* methods. With good quality crystal data and newer phasing programs,[6] an organic structure can be solved *without knowing any other information including molecular formula*, rendering NMR, MS, and IR necessary only for validation and data reporting requirements for routine elucidation.

A hallmark of SC-XRD is that the absolute stereochemistry of organic molecules can be established without ancillary methods via anomalous dispersion. In SC-XRD, diffraction images containing spots (a.k.a. reflections) are collected, and their processing affords an integrated list of thousands of unique reflections and their intensities prior to structure solution and refinement. These reflections are defined by their indices (h, k, l) in reciprocal space. For crystal systems that are chiral, reflection pairs with indices (h, k, l) and ($-h$, $-k$, $-l$), known as Friedel pairs or interchangeably as Bijvoet pairs in practice, exhibit small intensity differences due to anomalous dispersion (arising from inelastic interactions between atomic electrons and X-ray photons). These differences can be statistically analyzed in aggregate to yield absolute structure parameters (e.g., Flack/Parsons, Hooft),[7,8] where values near 0 with small standard uncertainty indicate correct modeling of absolute configuration in structure refinement. Two factors can amplify anomalous dispersion and thus increase confidence in (or permit) solving absolute structure: (1) the use of longer (low-energy) X-ray wavelengths and (2) the presence of heavy atoms. Since many synthetic molecules and natural products consist of only light atoms (C, H, N, O), less ubiquitous Cu Kα radiation (1.541 Å) must be used in very careful and lengthy data collection versus Mo Kα sources (0.711 Å) readily available at in-house diffractometers within chemistry facilities. Alternatively, heavy atoms can be introduced via derivatization (problematic if the sample is not readily modifiable or mass-limited), or by attempting cocrystallization with a heavy atom partner such as chlorinated solvent. If unsuccessful, then the compound will need to be cocrystallized with a chiral reference, or the crystal structure will provide *relative* stereochemistry, and methods that may be time-consuming must be used to establish the chirality of one stereocenter to assign full absolute structure (e.g., Mosher's or Marfey's analysis)[9,10] or to concurrently elucidate all stereocenters *de novo* (e.g., chiroptical analysis or total synthesis). Another approach involves imaging via scanning tunneling microscopy (STM) and atomic force microscopy (AFM).[11−17]

Despite the power of SC-XRD, the requirement of a suitable crystal can be a hurdle. Liquids or amorphous solids are typically excluded from analysis. Timely growth of suitable crystals is a task that is all but certain, especially for mass-limited samples. Isolated crystals may be of poor quality for SC-XRD due to excessive twinning, cracking, mosaicity, fragility, and desolvation. Visually acceptable crystals may diffract poorly (i.e., do not diffract to at least 0.84 Å resolution for chemical crystallography) due to excessive disorder, small size (microcrystals), or a nonideal crystal habit such as thin needles: factors that require synchrotron radiation or micro-crystal electron diffraction (MicroED).[18−20] Solved SC-XRD data may not be suitable for publication due to poor refinement statistics. Finally, a grown crystal may not be of the target; it may be an impurity such as a simple salt. One approach to bypass these limitations is to use a preformed crystalline matrix that can trap an organic compound and stabilize it via host−guest interactions followed by SC-XRD to ascertain target structure, thus effectively eliminating the uncertainty of growing an acceptable crystal of an organic compound.

DIVERSITY OF CRYSTALLINE MATRICES

Cocrystallization, where two or more compounds are incorporated into one lattice, is a long-standing strategy for crystallizing recalcitrant compounds. Examples of cocrystallants consist of supramolecular assemblies such as clathrates and container molecules.[2,21] While cocrystallization remains commonplace,[22] growing a diffraction-quality crystal is not guaranteed, or the isolated crystals may be solely of the cocrystallant. Postcrystallization methods involving crystalline matrices that can absorb organic compounds have been known[23−33] but have gained significant traction since the disclosure of the popular crystalline sponge method by Fujita et al. in 2013.[34] A discussion focusing upon preformed crystalline matrices, including their development, synthesis, advantages and limitations, application to organic structural problems, and perspectives on the future direction of this approach for organic structural elucidation, is presented herein.

Metal−Organic Frameworks. The most well-known strategy for organic structure determination using preformed matrices is the crystalline sponge method reported by Fujita and co-workers.[1−3,34−37] In the original 2013 report, a Zn(II) metal−organic framework (MOF), $\{[(ZnI_2)_3(tpt)_2]\cdot x(\text{solvent})\}_n$ (**1**) (tpt = tris(4-pyridyl)-1,3,5-triazine) is used, and its synthesis involves isolating crystals grown at the interface of layered solutions of tpt in $PhNO_2$ and ZnI_2 in MeOH at room temperature for 7 days (d), with soaking in cyclohexane at 50 °C for 7 d afterward to exchange strongly bound $PhNO_2$ (14 d total).[34,38] For inclusion, an analyte in μg to ng quantities dissolved in CH_2Cl_2 is added to **1** in cyclohexane followed by slow evaporation at 50 °C over 2 d. A salient feature of **1** is its heavy atoms, allowing absolute structure determination of guests with only light atoms using Mo Kα sources. The crystalline sponge method has since undergone development to enhance ease-of-use and improve crystallographic rigor to reduce the chance of structural errors (e.g., the misassignment of miyakosyne A).[39] In 2015, Clardy et al. reported an improved synthesis of **1** using a $CHCl_3$/MeOH layered system for crystallization, reducing synthetic time from 14 to 3 d.[40] The sponges were probed using synchrotron radiation; the trapping of neat guaiazulene, *trans*-anethole, and (1*R*)-(−)-menthyl acetate (absolute configuration solved) was analyzed, and crystallographic guidelines were established. Clardy et al. also examined changing the halide in **1** to Br or Cl

https://dx.doi.org/10.1021/acscentsci.0c01492
ACS Cent. Sci. 2021, 7, 406−414

to reduce X-ray scattering from the framework and increase guest visibility.[41] Another benefit observed for (1*R*)-(−)-menthyl acetate inclusion in the Br and Cl congeners was a reduction in structure refinement time from weeks to hours due to a smaller unit cell size and higher symmetry. Waldhart, Mankad, and Santarsiero used multiwell microplates to layer the crystallization solvents for **1** via a microwell droplet approach, leading to a higher yield of usable crystals in 10 h (exchange of $PhNO_2$ for cyclohexane can be done in 6 d if needed).[42] In 2017, Ramadhar, Clardy, et al. described a facile strategy for trapping solids and unstable liquids in **1** using methyl *tert*-butyl ether (MTBE) since polar solvents such as $CHCl_3$ adversely affect guest trapping.[43] Compounds soaked and observed via SC-XRD were *trans*-stilbene, vanillin, 4-trifluoromethylphenyl azide, and antimalarial drug (+)-artemisinin (**2**) (absolute configuration confirmed) (Figure 2). Using upgraded hardware at the NSF's ChemMatCARS beamline in the Advanced Photon Source at Argonne National Laboratory, data collection was completed in as little as 5 min.

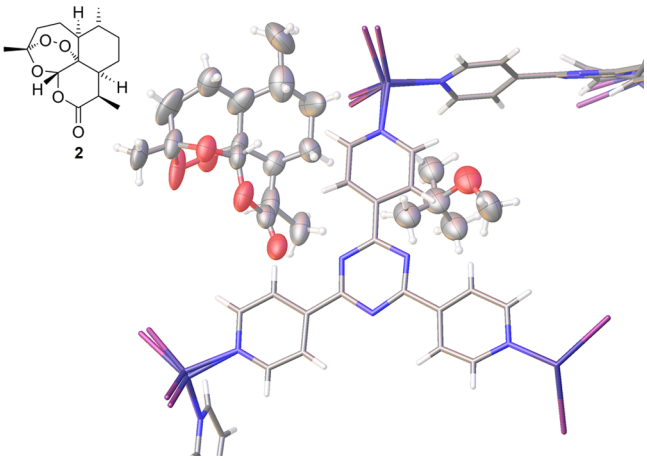

Figure 2. Inclusion of solid (+)-artemisinin (**2**) in **1** using MTBE solvent (CCDC 1545815). All guest thermal ellipsoids are displayed at the 50% probability level.

Since the inception of the crystalline sponge method, MOF **1** has found use in synthetic and mechanistic organic chemistry. Buchwald et al. revised an electrophilic hypervalent iodine trifluorothiomethylation reagent, where it was found to be a thioperoxide instead of a benziodoxole, thus helping to resolve the chemoselectivity of chlorobenziodoxole reactions with thiolates.[44] Sasai, Fujita, Rueping, et al. established the absolute configuration and regiochemistry of a product from a stereoselective phosphine-catalyzed β,γ-umpolung domino reaction of allenyl esters and dienones involving oxy-Michael and Rauhut-Currier processes.[45] Fujita et al. ascertained the absolute structure of an axially chiral molecule generated via C−H activation/asymmetric cross-coupling and a planar chiral molecule formed via asymmetric olefin metathesis[46] and subsequently investigated targets with chiral quaternary carbons.[47] Blackmond, Baran, Fujita, and co-workers resolved the regioselectivity of C−H-activated trifluoromethylation of a pyrrole and imidazole ring via electrochemical radical initiation of $Zn(SO_2CF_3)_2$.[48] Fujita et al. applied **1** in studies on oxygenated molecules: one involving regio- and stereoselectivity of epoxidations on α-humulene,[49] and another on ozonides.[50] Feringa, Houk, Fujita, and co-workers determined the structure of a chiral cyclohexene from a regioselective and enantiospecific formal [2,2]-dyotropic rearrangement of a homoallylic bromocycloheptene.[51] In 2020, Abe, Ohwada, Fujita, et al. solved the structure of indole-fused 6/5/8 tricycle **3** from a biocatalytic C−S bond formation with TleB, a CYP450 from *Streptomyces blastmyceticus* NBRC 12747, with the Cl congener of **1** (Figure 3).[52] Abe, Porco, Tantillo, Fujita,

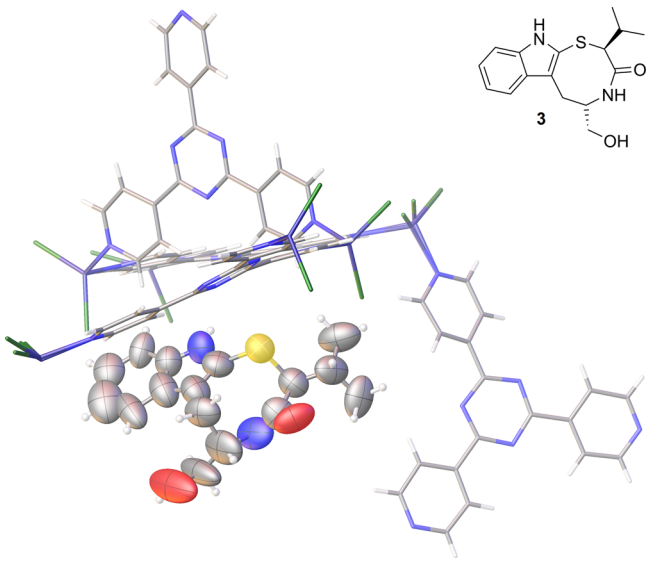

Figure 3. Incorporation of **3** within the Cl congener of **1** (CCDC 1941064). The most ordered guest is displayed; other guests and solvent molecules are hidden for clarity.

et al. used the same MOF to determine the structures of meroterpenoids chemoenzymatically synthesized using fungal meroterpenoid cyclases.[53] For mechanistic studies, Fujita et al. used a variant of **1** to examine Pd-catalyzed aryl brominations via SC-XRD.[54] ZnI_2, tpt, and a palladacycle (dibenzo[*f*,*h*]-quinolinyl Pd(II) methylxanthate) were cocrystallized, and subsequent solvent exchange with MeCN provided a crystalline flask for time-course studies that involved soaking with *N*-bromosuccinimide. An aryl−PdBr(MeCN) intermediate was observed prior to reductive elimination, showing that the reaction may not proceed solely via a Pd(IV)/Pd(II) cycle; a Pd(II)/Pd(0) route may also be operative. Fujita, Honda, and co-workers also used the crystalline flask approach to analyze a reversible thiol-Michael addition to cyanoenone drug candidate MCE-23.[55] In another case, Fernández, Fujita, et al. used **1** to observe that metal-free vicinal diborations of internal alkenes with bis(pinacolato)diboron (B_2pin_2) were likely occurring via a *syn*-addition manifold.[56]

The crystalline sponge method is especially alluring for mass-limited natural product and metabolite studies, with **1** and its Cl congener being used in multiple cases (Figure 4). Abe, Fujita, et al. elucidated astellifadiene (**4**), a mixed-bridged/fused tetracyclic sesterterpene from a terpene synthase genomically mined from *Emericella variecolor* NBRC 32302.[57] From Australian red alga *Laurencia elata*, the absolute structure of elatenyne (**5**) (a pseudo-*meso* bifuran)[58] and revised structures of cycloelatanenes A (**6**) and B (**7**) (epimeric C16 chamigrenes with a tricyclic spiro[5.5]undecene oxygen-bridged core)[59] were determined by Urban, Fujita, et al. They also revised the structure of fuliginone (**8**), a phenalenone from Australian plant *Macropidia fuliginosa*.[60] NMR and **1** were used by Weng, Fujita, and co-workers to

https://dx.doi.org/10.1021/acscentsci.0c01492
ACS Cent. Sci. 2021, 7, 406−414

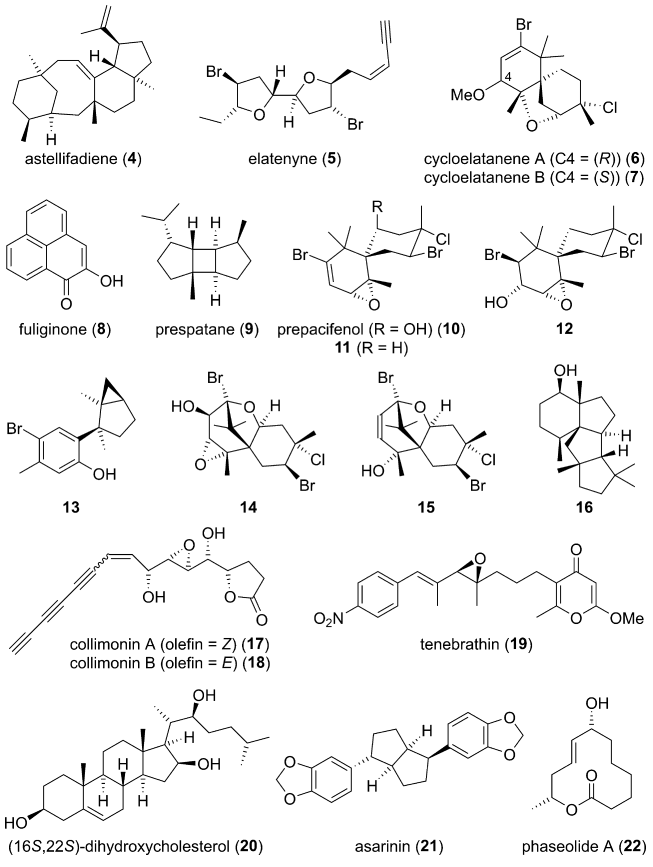

Figure 4. Structures from natural product studies solved with the aid of **1** or its Cl congener.

revise prespatane (**9**), a heterologously expressed fused tricyclic sesquiterpene from a red macroalga *Laurencia pacifica* sesquiterpene synthase.[61] Subsequent analysis of crude extracts from the same macroalga with **1** via a chemotyping workflow led to the resolution of six sesquiterpenes (**10**–**15**).[62] Genomic mining of *Penicillium chrysogenum* MT-12 by Abe, Fujita, et al. led to the isolation of mixed-spiro/fused tetracycle **16** from a heterologously expressed chimeric prenyltransferase-diterpene synthase, solved via the Cl congener of **1** since NMR analysis was difficult due to broadened line-shapes arising from conformational interconversion.[63] Kai, Fujita, et al. applied the same Cl-based sponge to determine the relative structure of click-derivatized collimonins A (**17**) and B (**18**), polyoxygenated hexadecanoic acids with an ene-triyne, from *Collimonas fungivorans* Ter 331.[64] In 2019, Abe, Fujita, et al. applied Cl-based **1** to solve tenebrathin (**19**), a γ-pyrone bearing a conjugated nitroaryl vinyl oxirane side chain from *Streptoalloteichus tenebrarius* NBRC 16177,[65] and Weng, Fujita, et al. elucidated intermediary (16*S*,22*S*)-dihydroxycholesterol (**20**) in a study on diosgenin plant biogenesis.[66] Di and co-workers determined the absolute structure of asarinin (**21**), a furofuran lignin from *Asarum heterotropoides* var. *mandshuricum* (*Xixin*) with synchrotron radiation and **1**.[67] Most recently, Morishita, Fujita, et al. solved phaseolide A (**22**), a 12-membered macrolactone genomically mined from *Macrophomina phaseolina*, using the Cl congener of **1**.[68] For metabolite analysis, Fujita et al. coupled HPLC with **1** to analyze reductive reactions on organic compounds by *Saccharomyces cerevisiae*.[69] In 2020, Badolo and co-workers demonstrated the proof-of-concept of applying **1** for drug metabolite studies when they analyzed the metabolism of gemfibrozil, a carboxylic acid bearing a hydrophobic chain, by rat and human liver microsomes and S9 fractions.[70]

While **1** has been extensively studied and applied,[71−83] it has its limitations. The maximum recommended guest size for **1** is 500 MW,[35] and it is incompatible with very basic/nucleophilic moieties and with highly polar solvents that may be needed for sufficient target solubilization. Not all targets may penetrate **1**, and those that do may not be adequately stabilized to afford acceptable refinement parameters for absolute structure determination or publication, or to even be observed and modeled. Modifications such as soaking at lower temperature and using the Cl congener of **1** allowed for the uptake of N-containing drug molecules (some with aliphatic/heterocyclic nitrogens, and others with inductively and mesomerically attenuated nitrogens).[84] Nonetheless, these limitations necessitate the design of new crystalline matrices. There have been reports on the design of new MOFs that leverage intermolecular interactions for guest ordering and have been used to trap solvent and small organic compounds.[85−89] A strategy to overcome guest disorder and incorporation issues is to use *coordinative* bonding to the MOF metal cluster. Coordinative alignment also increases guest bond length accuracy and confidence in atom assignment that may otherwise require complementary structural data. Yaghi et al. revealed that Al-based MOF-520 [$Al_8(\mu$–$OH)_8(HCOO)_4(btb)_4$ (btb = 1,3,5-benzenetribenzoate)] crystallizes into two enantiomorphs, yielding chiral MOFs that bind guests with alcohols and carboxylic acids at Al(III) (Figure 5).[90] They were also able to differentiate gibberellins

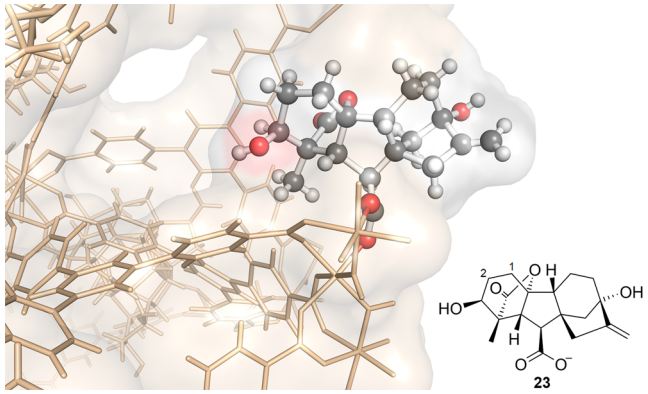

Figure 5. Use of coordinative alignment to trap gibberellin A_1 (**23**) in the Λ-enantiomorph of MOF-520 (CCDC 1488950). Another overlapping guest at a proximal Al(III) binding site in the periphery of the packing model is hidden for clarity.

A_1 (**23**) and A_3, which differ by an olefin at C1−C2. MOF-520 was recently expanded for azolates, sulfur oxoacids, and phosphorus oxoacids.[91] Other examples using coordinative alignment include Cu-based PCN-6 [$Cu_6(H_2O)_6(tatb)_4$·DMF·$12H_2O$ (tatb = 4,4′,4″-(1,3,5-triazine-2,4,6-triyl)tribenzoic acid)] by Pelagatti et al. for binding nicotine[92] and Mn-based CPF-5 ($Mn_{21}(HCOO)_{18}(H_2O)_{12}$(4-tetrazolate-benzoate)$_{12}$) by Cohen et al. for binding aliphatic, aryl, and heterocyclic amines.[93] In 2019, Gelder et al. demonstrated that the crystalline sponge method could be performed in water using lanthanide MOFs with btb or tatb ligands.[94] Carmalt and co-workers further demonstrated the capability of one of these lanthanide (Gd) MOFs to trap other aromatic targets

https://dx.doi.org/10.1021/acscentsci.0c01492
ACS Cent. Sci. 2021, 7, 406−414

including molinate, an aliphatic thiocarbamate herbicide.[95] For absolute structure determination, in cases where anomalous dispersion is insufficient due to high disorder, low incorporation, or data quality issues, MOFs with *reference* chiral motifs in the framework or trapped as a cocrystallant prior to soaking can be used. In this vein, Zaworotko and co-workers templated Co-MOFs with mandelate ligands for the inclusion of small chiral molecules.[96−98] Fujita and co-workers have used a Na-MOF with a *p*-phenylene-bridged dimannose ligand,[99] cocrystallized **1** with chiral triphenylene references,[100] and designed a Ag(I) MOF with peptide ligands to observe chiral alcohols and ketones along with desymmetrization of a *meso* compound and chiral hemiketal formation within the chiral environment of the MOF pores.[101] Pardo, Armentano, Ferrando-Soria, et al. used a Ca(II)/Cu(II) MOF with framework L-serine motifs to analyze vitamins C and B6, 17β-estradiol, and bupropion.[102] Finally, in addition to designing new MOFs, there may be MOFs in the literature that have not been investigated for the crystalline sponge method that may be viable.[103]

Coordination Cages. Metal−organic polyhedra (MOPs, a.k.a. coordination cages) can be thought of as analogous to cages in porous coordination polymers except without being interconnected by coordinative bonds. MOPs have long been investigated for guest binding applications.[104−106] Coordination cages as preformed crystalline matrices have recently been used for host−guest studies consistent with the crystalline sponge method.[107] When Ward et al. encountered difficulty in obtaining host−guest structures using a $[Co_8L_{12}](BF_4)_{16}$ cage with naphthyl-based bis-bidentate bridging ligands via cocrystallization, they used preformed crystals of the cage for soaking,[108] where neat cycloundecanone (with minimal MeOH to prevent crystal desolvation) was trapped and observed. Other studies with a similar cage led to the observation of adamantane-1-carboxylic acid and alkylphosphonate chemical warfare agent simulants via SC-XRD.[109,110] In 2020, Ward et al. used their Co-based coordination cages to demonstrate that various fused bicyclic aliphatic and aromatic guests including 4-methoxycoumarin (**24**) were incorporated into the cage in a 1:1 or 2:1 ratio (Figure 6),[111] and to probe cavity-based binding and external crystal surface interactions.[104] In these studies, crystals were soaked in neat liquid target or in a concentrated MeOH solution of target over 2 d, providing another way to analyze solids that require dissolution in polar protic solvents. For Co-based cage synthesis, upon performing a one-step synthesis of the bis-bidentate ligand, crystals can be conventionally grown in 7 d or in 12 h via a solvothermal method yielding higher-quality larger crystals.[112,113] Soaking experiments for MOPs have been reported in as short as a few minutes versus 2−4 d reported with MOFs,[107] providing another potential benefit of using MOPs.

Porous Organic Materials. Porous organic materials (POMs) (a.k.a. porous organic molecular crystals (POMCs)) are porous networks formed from organic molecules held together by intermolecular forces in the absence of extended covalent or coordination bonds.[114] POMs offer some advantages over inorganic-based materials for structure determination. Due to a lack of heavy atoms, X-ray scattering from the framework is reduced thus increasing guest visibility. Furthermore, the lack of labile metal−ligand bonds may make POMs amenable for nucleophilic and basic targets. POMs developed thus far as preformed crystalline matrices for

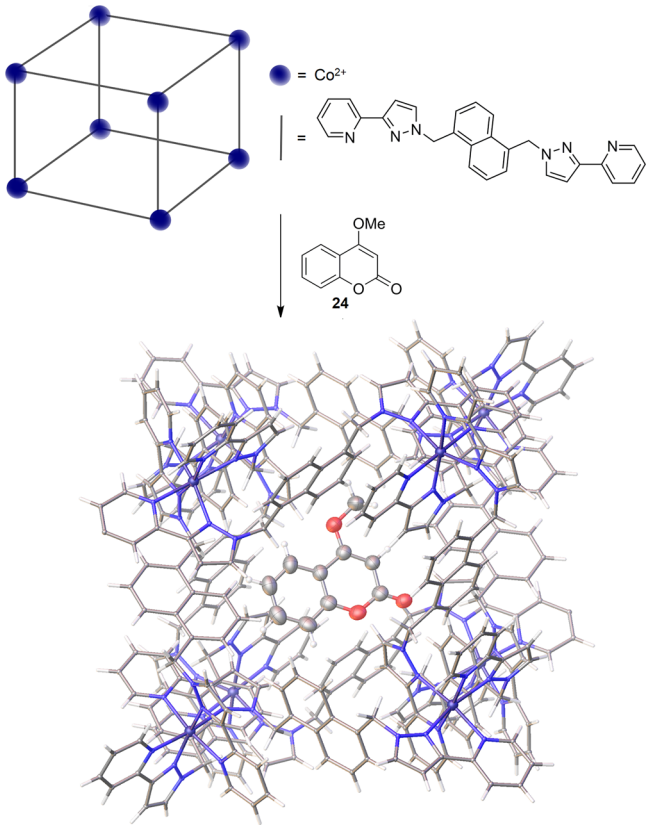

Figure 6. Trapping of 4-methoxycoumarin (**24**) in $[Co_8L_{12}]^{16+}$ (CCDC 1970071). While **24** is incorporated into the cage in a 2:1 ratio, the second guest molecule, positional disorder for each guest, and counterions are hidden for clarity.

structure elucidation are based on tetraimines or cyclophanes.[114−117] Costa et al. used a POM consisting of discrete cages of macrocyclic tetraimines for the elucidation of small organic compounds such as (*R*)-(+)-limonene and (*S*)-(−)-nicotine (**25**) (Figure 7).[114] These POMs were synthesized via Schiff base condensation and crystallization with a diamine and terephthaldehyde over 4−10 weeks. Solvent was removed *in vacuo*, with crystal porosity staying intact, prior to soaking with neat target from a few minutes to 2−3 d. The tetraimines were also used to study competitive sorption of phthalates,[115] and to view a rare C(sp^3)−F···F−

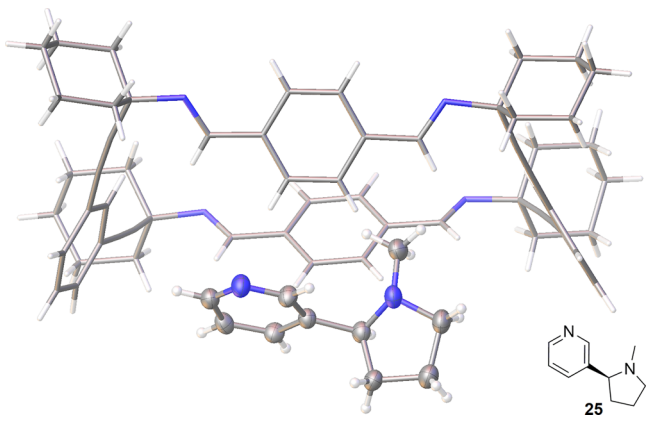

Figure 7. Incorporation of (*S*)-(−)-nicotine (**25**) in a macrocyclic tetraimine POM (CCDC 1063714). Disorder is hidden for clarity.

https://dx.doi.org/10.1021/acscentsci.0c01492
ACS Cent. Sci. 2021, 7, 406−414

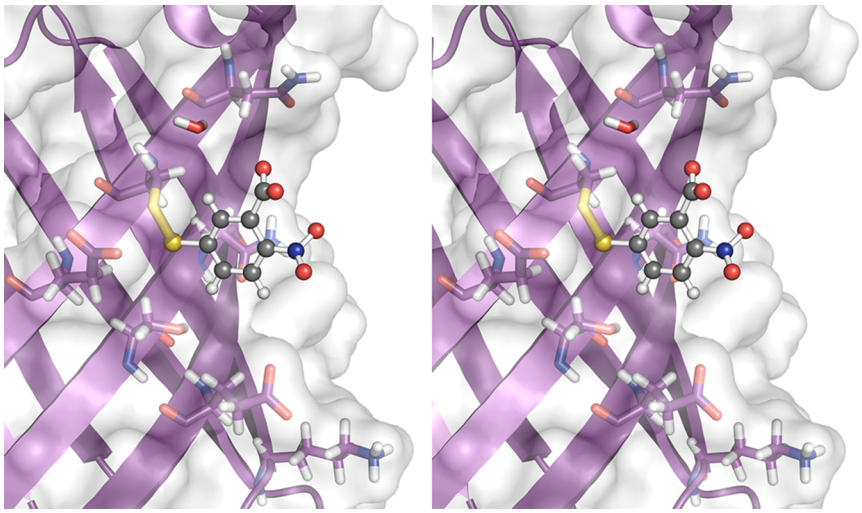

Figure 8. Wall-eyed stereo view of 5-mercapto-2-nitrobenzoic acid (**26**) in CJ N182C (PDB 5W3A). Proximal residues are displayed.

C(sp^3) interaction.[116] In 2020, Yamaguchi et al. reported the synthesis of adamantyl/tetrazinyl-based cyclophane POMs via S_NAr, slow evaporation, and vacuum treatment followed by trapping (in 24 h) and observation of neat green leaf volatiles *cis*-3-hexen-1-ol and *trans*-2-hexenal.[117] In regard to chirality determination, the absolute structures of (*R*)-(+)-limonene and **25** in the tetraimine POM were not solved due to the use of Mo Kα radiation; thus, unlike MOFs and MOPs, existing POMs will require Cu Kα radiation for chirality determination of light-atom guests.

Biological Scaffolds. The design of biologically based crystalline matrices for organic structure elucidation is in its infancy, with earlier studies focusing on fragment-based screening and combinatorial applications.[23,24] Macromolecular structures offer large binding sites that enable the possibility of trapping large molecules and other macromolecules.[118] In regard to organic molecules, Matsumoto et al. have described using multidrug resistance regulator protein, RamR, in a complementary strategy to the crystalline sponge method.[119] RamR, cloned from *Salmonella enterica* serovar Typhimurium (ATCC14028s) and recombinantly expressed in *Escherichia coli*,[120] was cocrystallized with ethidium bromide, cholic acid, and a synthetic intermediate of anticancer agent gefitinib, illustrating the flexibility of RamR to complex with non-native ligands. Snow and co-workers, inspired by the idea of covalent attachment,[90] used mutants of an engineered polyisoprenoid-binding protein from *Campylobacter jejuni* as a preformed crystalline matrix (CJ), featuring large (13 nm) solvent channels with proximal cysteine binding sites for guest conjugation (2 h soaking time).[121] Hydroxymercuribenzoate, monobromobimane, selenocysteine, and 5-mercapto-2-nitrobenzoic acid (**26**) were conjugated, with the latter being the most readily resolved (Figure 8). Recently, Yan et al. described a self-assembled 3D DNA crystal lattice with well-defined cavities that can potentially be used for target trapping, which remains to be seen for organic structural elucidation.[122] Finally, while the use of biological scaffolds is promising, especially for analysis of large molecules, the lower crystallographic resolution will increase the difficulty in modeling guests; thus, an abundance of caution during refinement must be exercised.[123−125]

OUTLOOK/PERSPECTIVE

The use of preformed crystalline matrices for structural elucidation in organic, medicinal, and chemical biology applications exhibits promise as a first-line technique; however, as with any method, further development to expand scope, robustness, and operational ease-of-use must be performed to realize that goal. Just as a variety of catalysts exist for cross-coupling reactions, it is unrealistic to rely upon **1** as a universal matrix. The sustained development and study of new and existing MOFs, MOPs, POMs, and biological scaffolds are important to expand the chemical space of analyzable targets. Preformed biologically based crystalline matrices provide an interesting avenue for trapping very large organic targets and macromolecules. It is important for those developing new matrices to collaborate with end users to identify unmet challenges and applications. For those interested in applying the method, the scope of successful inclusions indicate that it is a worthwhile endeavor. It must be noted that, just like any experiment, a trial-and-error approach may be required. Screening of various matrices and soaking conditions (e.g., solvent, temperature, duration, etc.) to optimize target inclusion and maximize guest occupancy will increase the chance of obtaining a quality structure. In addition, after soaking, it is necessary to assess crystals to find one of good quality (i.e., ones with suitable diffraction approaching 0.84 Å and with minimal to no defects such as cracking or twinning), which is best determined through examination of the diffraction images and viewing harvested indexed reflections in reciprocal space, to generate publishable crystallographic data that strongly supports a stated structural hypothesis.[40] It is also possible that inclusion of a desired target may not be possible with the current state-of-the-art; however, its *in crystallo* analysis may soon be reconciled with the design of new matrices. Finally, in light of the disorder issues that may arise in these systems, it is of paramount importance to enforce high crystallographic rigor and objectivity in data analysis and interpretation to preserve a pertinent idiom in chemistry, that "*seeing is believing*".[40,126]

https://dx.doi.org/10.1021/acscentsci.0c01492
ACS Cent. Sci. 2021, 7, 406−414

AUTHOR INFORMATION

Corresponding Author

Timothy R. Ramadhar − *Department of Chemistry, Howard University, Washington, DC 20059, United States;* orcid.org/0000-0002-7063-5445; Email: timothy.ramadhar@howard.edu

Author

Ashley D. Cardenal − *Department of Chemistry, Howard University, Washington, DC 20059, United States;* orcid.org/0000-0002-0639-8596

Complete contact information is available at: https://pubs.acs.org/10.1021/acscentsci.0c01492

Author Contributions

The manuscript was written through contributions of both authors. Both authors have given approval to the final version of the manuscript.

Notes

The authors declare no competing financial interest.

ACKNOWLEDGMENTS

T.R.R. gratefully acknowledges financial support from Pfizer Inc. (Groton, CT) and Howard University.

REFERENCES

(1) Gee, W. J. *Dalton Trans.* **2017**, *46*, 15979.
(2) Rissanen, K. *Chem. Soc. Rev.* **2017**, *46*, 2638.
(3) Du, Q.; Peng, J.; Wu, P.; He, H. *TrAC, Trends Anal. Chem.* **2018**, *102*, 290.
(4) Burns, D. C.; Mazzola, E. P.; Reynolds, W. F. *Nat. Prod. Rep.* **2019**, *36*, 919.
(5) Liu, Y.; Saurí, J.; Mevers, E.; Peczuh, M. W.; Hiemstra, H.; Clardy, J.; Martin, G. E.; Williamson, R. T. *Science* **2017**, *356*, eaam5349.
(6) Sheldrick, G. M. *Acta Crystallogr., Sect. A: Found. Adv.* **2015**, *71*, 3.
(7) Parsons, S.; Flack, H. D.; Wagner, T. *Acta Crystallogr., Sect. B: Struct. Sci., Cryst. Eng. Mater.* **2013**, *B69*, 249.
(8) Hooft, R. W. W.; Straver, L. H.; Spek, A. L. *J. Appl. Crystallogr.* **2008**, *41*, 96.
(9) Hoye, T. R.; Jeffrey, C. S.; Shao, F. *Nat. Protoc.* **2007**, *2*, 2451.
(10) Bhushan, R.; Brückner, H. *J. Chromatogr. B: Anal. Technol. Biomed. Life Sci.* **2011**, *879*, 3148.
(11) Lopinski, G. P.; Moffatt, D. J.; Wayner, D. D. M.; Wolkow, R. A. *Nature* **1998**, *392*, 909.
(12) Böhringer, M.; Morgenstern, K.; Schneider, W.-D.; Berndt, R. *Angew. Chem., Int. Ed.* **1999**, *38*, 821.
(13) Kühnle, A.; Linderoth, T. R.; Hammer, B.; Besenbacher, F. *Nature* **2002**, *415*, 891.
(14) Ernst, K.-H.; Baumann, S.; Lutz, C. P.; Seibel, J.; Zoppi, L.; Heinrich, A. *Nano Lett.* **2015**, *15*, 5388.
(15) Stetsovych, O.; Švec, M.; Vacek, J.; Chocholoušová, J. V.; Jančařík, A.; Rybáček, J.; Kosmider, K.; Stará, I. G.; Jelínek, P.; Starý, I. *Nat. Chem.* **2017**, *9*, 213.
(16) Shiotari, A.; Tanaka, K.; Nakae, T.; Mori, S.; Okujima, T.; Uno, H.; Sakaguchi, H.; Sugimoto, Y. *J. Phys. Chem. C* **2018**, *122*, 4997.
(17) Ebeling, D.; Šekutor, M.; Stiefermann, M.; Tschakert, J.; Dahl, J. E. P.; Carlson, R. M. K.; Schirmeisen, A.; Schreiner, P. R. *Nat. Commun.* **2018**, *9*, 2420.
(18) Clegg, W. *Philos. Trans. R. Soc., A* **2019**, *377*, 20180239.
(19) Xu, W.; Lapidus, S. H.; Yakovenko, A. Y.; Kim, Y.; Borkiewicz, O. J.; Wiaderek, K. M.; Chen, Y.-S.; Kinnibrugh, T. L. Synchrotron X-ray Diffraction Applications. In *Materials Characterization*, 2019 ed.; ASM Handbook; ASM International, 2019; Vol. *10*, p 478.
(20) Danelius, E.; Halaby, S.; van der Donk, W. A.; Gonen, T. *Nat. Prod. Rep.* **2021**, in press. DOI: 10.1039/D0NP00035C.
(21) Byrn, M. P.; Curtis, C. J.; Hsiou, Y.; Khan, S. I.; Sawin, P. A.; Tendick, S. K.; Terzis, A.; Strouse, C. E. *J. Am. Chem. Soc.* **1993**, *115*, 9480.
(22) Li, Y.; Tang, S.; Yusov, A.; Rose, J.; Borrfors, A. N.; Hu, C. T.; Ward, M. D. *Nat. Commun.* **2019**, *10*, 4477.
(23) Carr, R.; Jhoti, H. *Drug Discovery Today* **2002**, *7*, 522.
(24) Congreve, M. S.; Davis, D. J.; Devine, L.; Granata, C.; O'Reilly, M.; Wyatt, P. G.; Jhoti, H. *Angew. Chem., Int. Ed.* **2003**, *42*, 4479.
(25) Ohmori, O.; Kawano, M.; Fujita, M. *J. Am. Chem. Soc.* **2004**, *126*, 16292.
(26) Bradshaw, D.; Claridge, J. B.; Cussen, E. J.; Prior, T. J.; Rosseinsky, M. *Acc. Chem. Res.* **2005**, *38*, 273.
(27) Kawano, M.; Fujita, M. *Coord. Chem. Rev.* **2007**, *251*, 2592.
(28) Kawamichi, T.; Kodama, T.; Kawano, M.; Fujita, M. *Angew. Chem., Int. Ed.* **2008**, *47*, 8030.
(29) Kawamichi, T.; Haneda, T.; Kawano, M.; Fujita, M. *Nature* **2009**, *461*, 633.
(30) Inokuma, Y.; Arai, T.; Fujita, M. *Nat. Chem.* **2010**, *2*, 780.
(31) Ohara, K.; Kawano, M.; Inokuma, Y.; Fujita, M. *J. Am. Chem. Soc.* **2010**, *132*, 30.
(32) Nassimbeni, L. R.; Su, H. *CrystEngComm* **2013**, *15*, 7396.
(33) Inokuma, Y.; Fujita, M. *Bull. Chem. Soc. Jpn.* **2014**, *87*, 1161.
(34) Inokuma, Y.; Yoshioka, S.; Ariyoshi, J.; Arai, T.; Hitora, Y.; Takada, K.; Matsunaga, S.; Rissanen, K.; Fujita, M. *Nature* **2013**, *495*, 461.
(35) Inokuma, Y.; Yoshioka, S.; Ariyoshi, J.; Arai, T.; Fujita, M. *Nat. Protoc.* **2014**, *9*, 246.
(36) Hoshino, M.; Khutia, A.; Xing, H.; Inokuma, Y.; Fujita, M. *IUCrJ* **2016**, *3*, 139.
(37) Stallforth, P.; Clardy, J. *Nature* **2013**, *495*, 456.
(38) Biradha, K.; Fujita, M. *Angew. Chem., Int. Ed.* **2002**, *41*, 3392.
(39) Inokuma, Y.; Yoshioka, S.; Ariyoshi, J.; Arai, T.; Hitora, Y.; Takada, K.; Matsunaga, S.; Rissanen, K.; Fujita, M. *Nature* **2013**, *501*, 262.
(40) Ramadhar, T. R.; Zheng, S.-L.; Chen, Y.-S.; Clardy, J. *Acta Crystallogr., Sect. A: Found. Adv.* **2015**, *A71*, 46.
(41) Ramadhar, T. R.; Zheng, S.-L.; Chen, Y.-S.; Clardy, J. *Chem. Commun.* **2015**, *51*, 11252.
(42) Waldhart, G. W.; Mankad, N. P.; Santarsiero, B. D. *Org. Lett.* **2016**, *18*, 6112.
(43) Ramadhar, T. R.; Zheng, S.-L.; Chen, Y.-S.; Clardy, J. *CrystEngComm* **2017**, *19*, 4528.
(44) Vinogradova, E. V.; Müller, P.; Buchwald, S. L. *Angew. Chem., Int. Ed.* **2014**, *53*, 3125.
(45) Takizawa, S.; Kishi, K.; Yoshida, Y.; Mader, S.; Arteaga, F. A.; Lee, S.; Hoshino, M.; Rueping, M.; Fujita, M.; Sasai, H. *Angew. Chem., Int. Ed.* **2015**, *54*, 15511.
(46) Yoshioka, S.; Inokuma, Y.; Hoshino, M.; Sato, T.; Fujita, M. *Chem. Sci.* **2015**, *6*, 3765.
(47) Sairenji, S.; Kikuchi, T.; Abozeid, M. A.; Takizawa, S.; Sasai, H.; Ando, Y.; Ohmatsu, K.; Ooi, T.; Fujita, M. *Chem. Sci.* **2017**, *8*, 5132.
(48) O'Brien, A. G.; Maruyama, A.; Inokuma, Y.; Fujita, M.; Baran, P. S.; Blackmond, D. G. *Angew. Chem., Int. Ed.* **2014**, *53*, 11868.
(49) Zigon, N.; Hoshino, M.; Yoshioka, S.; Inokuma, Y.; Fujita, M. *Angew. Chem., Int. Ed.* **2015**, *54*, 9033.
(50) Yoshioka, S.; Inokuma, Y.; Duplan, V.; Dubey, R.; Fujita, M. *J. Am. Chem. Soc.* **2016**, *138*, 10140.
(51) Goh, S. S.; Champagne, P. A.; Guduguntla, S.; Kikuchi, T.; Fujita, M.; Houk, K. N.; Feringa, B. L. *J. Am. Chem. Soc.* **2018**, *140*, 4986.
(52) Morita, I.; Mori, T.; Mitsuhashi, T.; Hoshino, S.; Taniguchi, Y.; Kikuchi, T.; Nagae, K.; Nasu, N.; Fujita, M.; Ohwada, T.; Abe, I. *Angew. Chem., Int. Ed.* **2020**, *59*, 3988.
(53) Mitsuhashi, T.; Barra, L.; Powers, Z.; Kojasoy, V.; Cheng, A.; Yang, F.; Taniguchi, Y.; Kikuchi, T.; Fujita, M.; Tantillo, D. J.; Porco, J. A., Jr.; Abe, I. *Angew. Chem., Int. Ed.* **2020**, *59*, 23772.

(54) Ikemoto, K.; Inokuma, Y.; Rissanen, K.; Fujita, M. *J. Am. Chem. Soc.* **2014**, *136*, 6892.
(55) Duplan, V.; Hoshino, M.; Li, W.; Honda, T.; Fujita, M. *Angew. Chem., Int. Ed.* **2016**, *55*, 4919.
(56) Cuenca, A. B.; Zigon, N.; Duplan, V.; Hoshino, M.; Fujita, M.; Fernández, E. *Chem. - Eur. J.* **2016**, *22*, 4723.
(57) Matsuda, Y.; Mitsuhashi, T.; Lee, S.; Hoshino, M.; Mori, T.; Okada, M.; Zhang, H.; Hayashi, F.; Fujita, M.; Abe, I. *Angew. Chem., Int. Ed.* **2016**, *55*, 5785.
(58) Urban, S.; Brkljača, R.; Hoshino, M.; Lee, S.; Fujita, M. *Angew. Chem., Int. Ed.* **2016**, *55*, 2678.
(59) Lee, S.; Hoshino, M.; Fujita, M.; Urban, S. *Chem. Sci.* **2017**, *8*, 1547.
(60) Brkljača, R.; Schneider, B.; Hidalgo, W.; Otálvaro, F.; Ospina, F.; Lee, S.; Hoshino, M.; Fujita, M.; Urban, S. *Molecules* **2017**, *22*, 211.
(61) Kersten, R. D.; Lee, S.; Fujita, D.; Pluskal, T.; Kram, S.; Smith, J. E.; Iwai, T.; Noel, J. P.; Fujita, M.; Weng, J.-K. *J. Am. Chem. Soc.* **2017**, *139*, 16838.
(62) Wada, N.; Kersten, R. D.; Iwai, T.; Lee, S.; Sakurai, F.; Kikuchi, T.; Fujita, D.; Fujita, M.; Weng, J.-K. *Angew. Chem., Int. Ed.* **2018**, *57*, 3671.
(63) Mitsuhashi, T.; Kikuchi, T.; Hoshino, S.; Ozeki, M.; Awakawa, T.; Shi, S.-P.; Fujita, M.; Abe, I. *Org. Lett.* **2018**, *20*, 5606.
(64) Kai, K.; Sogame, M.; Sakurai, F.; Nasu, N.; Fujita, M. *Org. Lett.* **2018**, *20*, 3536.
(65) Hoshino, S.; Mitsuhashi, T.; Kikuchi, T.; Wong, C. P.; Morita, H.; Awakawa, T.; Fujita, M.; Abe, I. *Org. Lett.* **2019**, *21*, 6519.
(66) Christ, B.; Xu, C.; Xu, M.; Li, F.-S.; Wada, N.; Mitchell, A. J.; Han, X.-L.; Wen, M.-L.; Fujita, M.; Weng, J.-K. *Nat. Commun.* **2019**, *10*, 3206.
(67) Li, K.; Yang, D.-S.; Gu, X.-F.; Di, B. *Fitoterapia* **2019**, *134*, 135.
(68) Morishita, Y.; Sonohara, T.; Taniguchi, T.; Adachi, K.; Fujita, M.; Asai, T. *Org. Biomol. Chem.* **2020**, *18*, 2813.
(69) Inokuma, Y.; Ukegawa, T.; Hoshino, M.; Fujita, M. *Chem. Sci.* **2016**, *7*, 3910.
(70) Rosenberger, L.; von Essen, C.; Khutia, A.; Kühn, C.; Urbahns, K.; Georgi, K.; Hartmann, R. W.; Badolo, L. *Drug Metab. Dispos.* **2020**, *48*, 587.
(71) Ohara, K.; Nakai, A.; Yamaguchi, K. *Eur. J. Mass Spectrom.* **2015**, *21*, 413.
(72) Gu, X.-F.; Zhao, Y.; Li, K.; Su, M.-X.; Yan, F.; Li, B.; Du, Y.-X.; Di, B. *J. Chromatogr. A* **2016**, *1474*, 130.
(73) Kawahata, M.; Komagawa, S.; Ohara, K.; Fujita, M.; Yamaguchi, K. *Tetrahedron Lett.* **2016**, *57*, 4633.
(74) Hayes, L. M.; Knapp, C. E.; Nathoo, K. Y.; Press, N. J.; Tocher, D. A.; Carmalt, C. J. *Cryst. Growth Des.* **2016**, *16*, 3465.
(75) Hayes, L. M.; Press, N. J.; Tocher, D. A.; Carmalt, C. J. *Cryst. Growth Des.* **2017**, *17*, 858.
(76) Brunet, G.; Safin, D. A.; Robeyns, K.; Facey, G. A.; Korobkov, I.; Filinchuk, Y.; Murugesu, M. *Chem. Commun.* **2017**, *53*, 5645.
(77) Zigon, N.; Kikuchi, T.; Ariyoshi, J.; Inokuma, Y.; Fujita, M. *Chem. - Asian J.* **2017**, *12*, 1057.
(78) Hayashi, Y.; Ohara, K.; Taki, R.; Saeki, T.; Yamaguchi, K. *Analyst* **2018**, *143*, 1475.
(79) de Poel, W.; Tinnemans, P. T.; Duchateau, A. L. L.; Honing, M.; Rutjes, F. P. J. T.; Vlieg, E.; de Gelder, R. *Cryst. Growth Des.* **2018**, *18*, 126.
(80) Siskos, M. G.; Choudhary, M. I.; Gerothanassis, I. P. *Tetrahedron* **2018**, *74*, 4728.
(81) Hayashi, Y.; Ohara, K.; Taki, R.; Saeki, T.; Yamaguchi, K. *Anal. Chim. Acta* **2019**, *1064*, 80.
(82) Yuan, L.; Li, S.; Pan, F. *Inorg. Chem.* **2019**, *58*, 7649.
(83) Habib, F.; Tocher, D. A.; Press, N. J.; Carmalt, C. J. *Microporous Mesoporous Mater.* **2020**, *308*, 110548.
(84) Sakurai, F.; Khutia, A.; Kikuchi, T.; Fujita, M. *Chem. - Eur. J.* **2017**, *23*, 15035.
(85) Gao, H. Y.; Zhang, L.; Yan, C. S.; Meng, L. N.; Li, J. Q.; Meng, P. P.; Gong, L. L.; Luo, F. *CrystEngComm* **2016**, *18*, 5429.
(86) Yang, X.-Y.; Yuan, S.; Qin, J.-S.; Lollar, C.; Alsalme, A.; Zhou, H.-C. *Mater. Chem. Front.* **2017**, *1*, 1764.
(87) Choi, D.; Lee, H.; Lee, J. J.; Jung, O.-S. *Cryst. Growth Des.* **2017**, *17*, 6677.
(88) Balestri, D.; Mazzeo, P. P.; Carraro, C.; Demitri, N.; Pelagatti, P.; Bacchi, A. *Angew. Chem., Int. Ed.* **2019**, *58*, 17342.
(89) Qiu, Q.-F.; Chen, C.-X.; Wei, Z.-W.; Cao, C.-C.; Zhu, N.-X.; Wang, H.-P.; Wang, D.; Jiang, J.-J.; Su, C.-Y. *Inorg. Chem.* **2019**, *58*, 61.
(90) Lee, S.; Kapustin, E. A.; Yaghi, O. M. *Science* **2016**, *353*, 808.
(91) Pei, X.; Bürgi, H.-B.; Kapustin, E. A.; Liu, Y.; Yaghi, O. M. *J. Am. Chem. Soc.* **2019**, *141*, 18862.
(92) Balestri, D.; Capucci, D.; Demitri, N.; Bacchi, A.; Pelagatti, P. *Materials* **2017**, *10*, 727.
(93) Wang, L.; Moore, C. E.; Cohen, S. M. *Cryst. Growth Des.* **2017**, *17*, 6174.
(94) de Poel, W.; Tinnemans, P.; Duchateau, A. L. L.; Honing, M.; Rutjes, F. P. J. T.; Vlieg, E.; de Gelder, R. *Chem. - Eur. J.* **2019**, *25*, 14999.
(95) Lunn, R. D. J.; Tocher, D. A.; Sidebottom, P. J.; Montgomery, M. G.; Keates, A. C.; Carmalt, C. J. *Cryst. Growth Des.* **2020**, *20*, 7238.
(96) Zhang, S.-Y.; Wojtas, L.; Zaworotko, M. J. *J. Am. Chem. Soc.* **2015**, *137*, 12045.
(97) Zhang, S.-Y.; Yang, C.-X.; Shi, W.; Yan, X.-P.; Cheng, P.; Wojtas, L.; Zaworotko, M. J. *Chem.* **2017**, *3*, 281.
(98) Zhang, S.-Y.; Fairen-Jimenez, D.; Zaworotko, M. J. *Angew. Chem., Int. Ed.* **2020**, *59*, 17600.
(99) Ning, G.-H.; Matsumura, K.; Inokuma, Y.; Fujita, M. *Chem. Commun.* **2016**, *52*, 7013.
(100) Yan, K.; Dubey, R.; Arai, T.; Inokuma, Y.; Fujita, M. *J. Am. Chem. Soc.* **2017**, *139*, 11341.
(101) Saito, A.; Sawada, T.; Fujita, M. *Angew. Chem., Int. Ed.* **2020**, *59*, 20367.
(102) Mon, M.; Bruno, R.; Ferrando-Soria, J.; Bartella, L.; Di Donna, L.; Talia, M.; Lappano, R.; Maggiolini, M.; Armentano, D.; Pardo, E. *Mater. Horiz.* **2018**, *5*, 683.
(103) Inokuma, Y.; Matsumura, K.; Yoshioka, S.; Fujita, M. *Chem. - Asian J.* **2017**, *12*, 208.
(104) Taylor, C. G. P.; Train, J. S.; Ward, M. D. *Chemistry* **2020**, *2*, 510.
(105) Ajami, D.; Liu, L.; Rebek, J., Jr. *Chem. Soc. Rev.* **2015**, *44*, 490.
(106) Tabacchi, G. *ChemPhysChem* **2018**, *19*, 1249.
(107) Ward, M. D.; Hunter, C. A.; Williams, N. H. *Chem. Lett.* **2017**, *46*, 2.
(108) Turega, S.; Cullen, W.; Whitehead, M.; Hunter, C. A.; Ward, M. D. *J. Am. Chem. Soc.* **2014**, *136*, 8475.
(109) Cullen, W.; Turega, S.; Hunter, C. A.; Ward, M. D. *Chem. Sci.* **2015**, *6*, 625.
(110) Taylor, C. G. P.; Piper, J. R.; Ward, M. D. *Chem. Commun.* **2016**, *52*, 6225.
(111) Taylor, C. G. P.; Argent, S. P.; Ludden, M. D.; Piper, J. R.; Mozaceanu, C.; Barnett, S. A.; Ward, M. D. *Chem. - Eur. J.* **2020**, *26*, 3054.
(112) Whitehead, M.; Turega, S.; Stephenson, A.; Hunter, C. A.; Ward, M. D. *Chem. Sci.* **2013**, *4*, 2744.
(113) Tidmarsh, I. S.; Faust, T. B.; Adams, H.; Harding, L. P.; Russo, L.; Clegg, W.; Ward, M. D. *J. Am. Chem. Soc.* **2008**, *130*, 15167.
(114) Sanna, E.; Escudero-Adán, E. C.; Bauzá, A.; Ballester, P.; Frontera, A.; Rotger, C.; Costa, A. *Chem. Sci.* **2015**, *6*, 5466.
(115) Sanna, E.; Escudero-Adán, E. C.; López, C.; Ballester, P.; Rotger, C.; Costa, A. *J. Org. Chem.* **2016**, *81*, 5173.
(116) Sanna, E.; Bauzá, A.; Escudero-Adán, E. C.; Rotger, C.; Frontera, A.; Costa, A. *Cryst. Growth Des.* **2017**, *17*, 3611.
(117) Tominaga, M.; Hyodo, T.; Maekawa, Y.; Kawahata, M.; Yamaguchi, K. *Chem. - Eur. J.* **2020**, *26*, 5157.
(118) Ward, A. R.; Snow, C. D. *Curr. Opin. Struct. Biol.* **2020**, *60*, 85.
(119) Matsumoto, T.; Nakashima, R.; Yamano, A.; Nishino, K. *Biochem. Biophys. Res. Commun.* **2019**, *518*, 402.

https://dx.doi.org/10.1021/acscentsci.0c01492
ACS Cent. Sci. 2021, 7, 406−414

(120) Yamasaki, S.; Nikaido, E.; Nakashima, R.; Sakurai, K.; Fujiwara, D.; Fujii, I.; Nishino, K. *Nat. Commun.* **2013**, *4*, 2078.
(121) Huber, T. R.; McPherson, E. C.; Keating, C. E.; Snow, C. D. *Bioconjugate Chem.* **2018**, *29*, 17.
(122) Zhang, F.; Simmons, C. R.; Gates, J.; Liu, Y.; Yan, H. *Angew. Chem., Int. Ed.* **2018**, *57*, 12504.
(123) Liebeschuetz, J.; Hennemann, J.; Olsson, T.; Groom, C. R. *J. Comput.-Aided Mol. Des.* **2012**, *26*, 169.
(124) Deller, M. C.; Rupp, B. *J. Comput.-Aided Mol. Des.* **2015**, *29*, 817.
(125) Wlodawer, A.; Dauter, Z.; Porebski, P. J.; Minor, W.; Stanfield, R.; Jaskolski, M.; Pozharski, E.; Weichenberger, C. X.; Rupp, B. *FEBS J.* **2018**, *285*, 444.
(126) Campbell, M. G.; Powers, T. M.; Zheng, S.-L. *J. Chem. Educ.* **2016**, *93*, 270.

https://dx.doi.org/10.1021/acscentsci.0c01492
ACS Cent. Sci. 2021, 7, 406−414